Measuring the Polarizabilities of Neutral and Charged Pions at JLab

Victor Tarasov

NRC KI

for the CPP/NPP collaboration

ICPPA-7, October 22-25, 2024, Moscow, Russia

Layout

- Polarizability of the charged and neutral pions
- Motivation
- Previous measurements
- Experimental setup
- Current status of the CPP/NPP experiments
- Conclusion

Polarizability of particles

Polarizability is a value that determines how strongly a particle is deformed in an external electric field.

Polarizability is a proportionality coefficient, which has the dimension of volume, between the magnitude of the applied external field strength and the magnitude of the dipole moment induced by it.

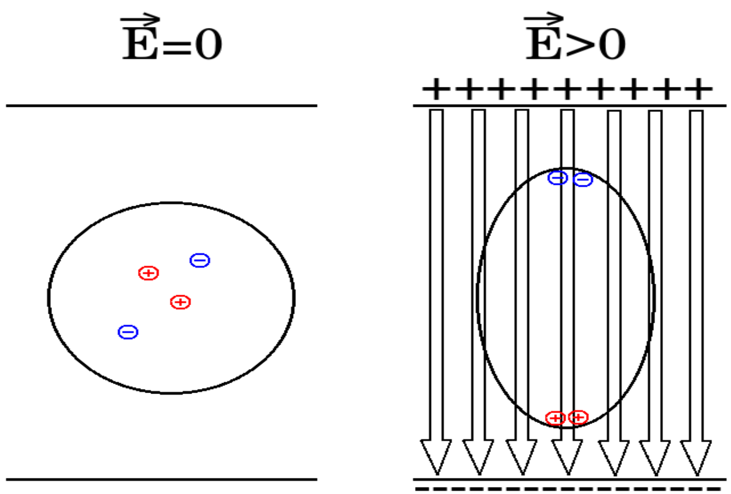

E ≈ 0.1 GeV/1 fm = 10^{23} Volt/m

$$\vec{p} = -\alpha \vec{E}$$

$$\vec{\mu} = \beta \vec{H}$$

Electric polarizability α ≈ 10^{-4} • Volume

Magnetic polarizability β ≈ 10^{-4} • Volume

The polarizability of pions characterizes their deformation in an external electromagnetic field

Pions polarizability

Polarizability is a fundamental property of hadrons.
The pion is the lightest known particle involved in the strong interaction.
Measuring the polarizability of the pion is an important test of fundamental symmetries at low energy QCD.

Predictions for polarizability of charged pions[1-3]:

$$\alpha_{\pi^+} = -\beta_{\pi^+} = \frac{4\alpha}{m_\pi F_\pi^2}(L_9^r - L_{10}^r)$$

$$\alpha_{\pi^+} - \beta_{\pi^+} = (5.7 \pm 1.0) \times 10^{-4} fm^3$$

For neutral pions[4-5]:

$$\alpha_{\pi^0} = -\beta_{\pi^0} = -\frac{\alpha}{96\pi^2 m_\pi F_\pi^2}$$

$$\alpha_{\pi^0} - \beta_{\pi^0} = (-1.9 \pm 0.2) \times 10^{-4} fm^3$$

where m_π is the pion mass, F_π is the pion decay constant, α — fine structure constant , L^r_9 and L^r_{10} are low energy constants in the Lagrangian.
Precision measurement of the polarizabilities of charged and neutral pions will allow us to obtain the parameters α_π and β_π with an accuracy of 10%, which exceeds the accuracy of all measurements existing today.

The pion polarizability also plays an important role in the (g − 2) μ anomaly [6], the interest in measuring which has grown since it was recently reported 4.2 standard deviations from the Standard Model prediction [7].

[1] Burgi U. // Nucl. Phys. B. 479. 392. (1996).
[2] Gasser J., Ivanov M.A., Sainio M.E. // Nucl. Phys. B. 745. 84. (2006).
[3] Pasquini B., Drechsel D., Scherer S. // Phys. Rev. C. 77. 065211. (2008).
[4] Babusci D., Belucci S., Giordano G. et al. // Phys. Lett. B. 277. 158. (1992).
[5] Bellucci S., Gasser J., Sainio M.E. // Nucl. Phys. B. 423. 80. (1994).
[6] Engel K., Patel H., Ramsey-Musolf M. // Phys. Rev. D. 86. 037502. (2012).
[7] Abi B., Albahri T., Al-Kilani S. et al. // Phys. Rev. Lett. 126. 141801. (2021).

Previous measurements of the pion polarizability

Charged pion polarizability (CPP)

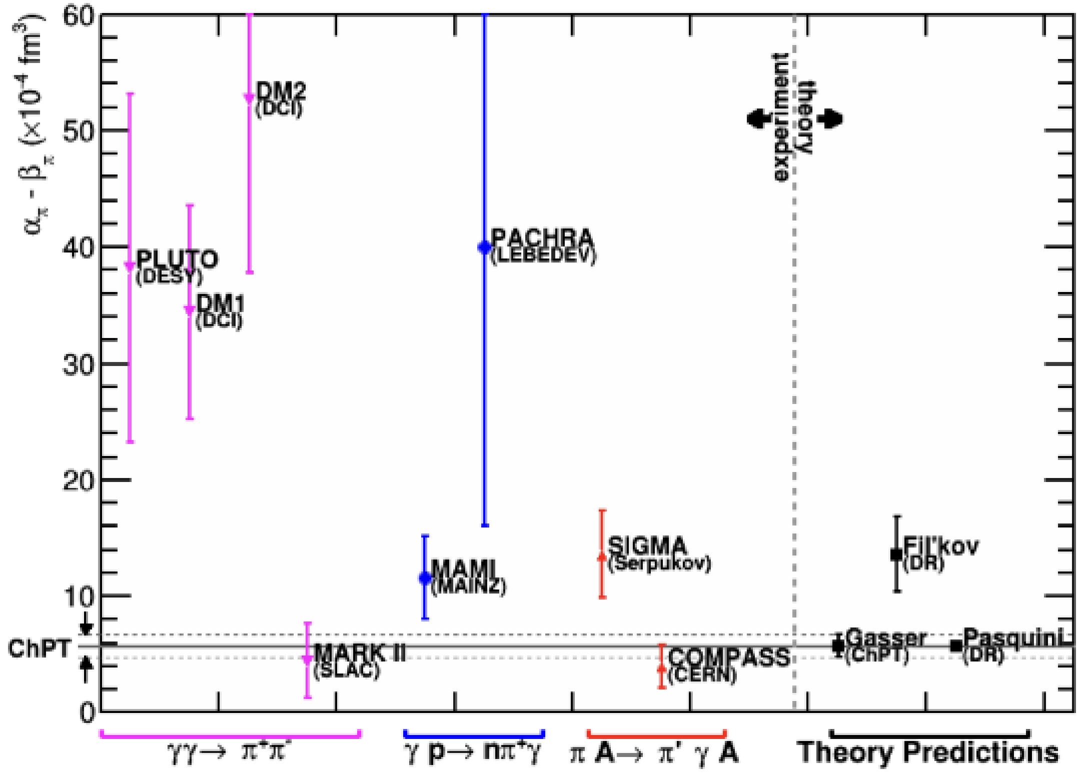

The charged pion polarizability $\alpha_{\pi+}$- $\beta_{\pi+}$ was measured by three different methods.
The most up to date measurement in each type are: MARK-II, MAMI, COMPASS.
The CPP measurement is expected to be 1.5 times better than the most accurate one available today.

Previous measurements and expected data for charged(left) and neutral(right) pions

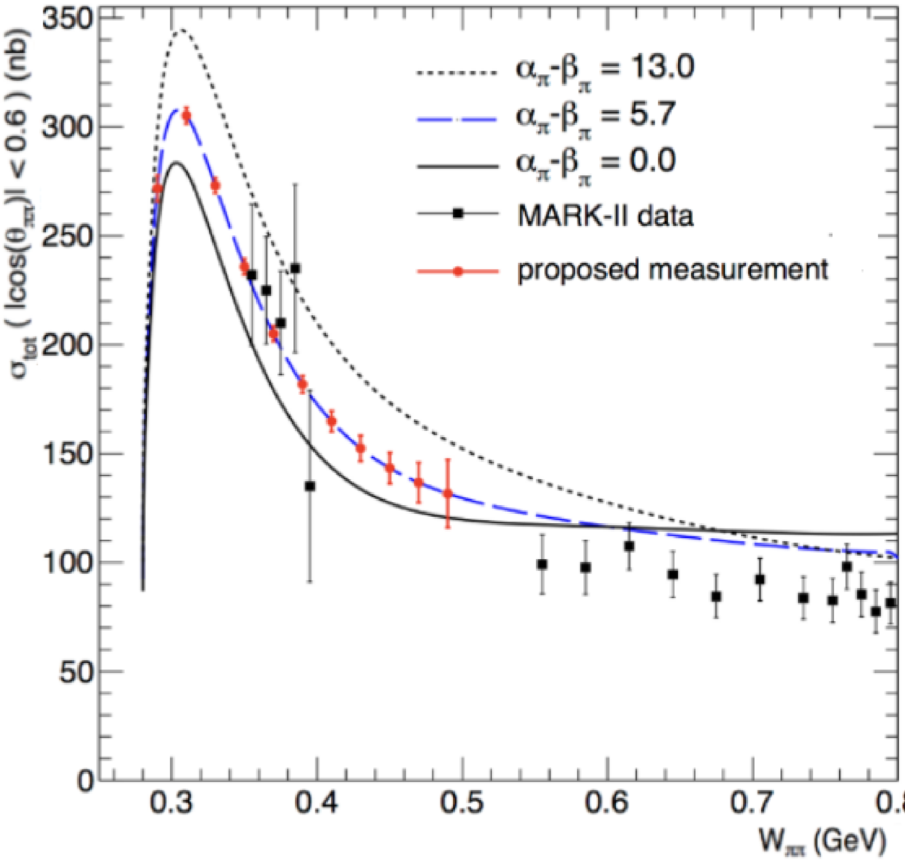

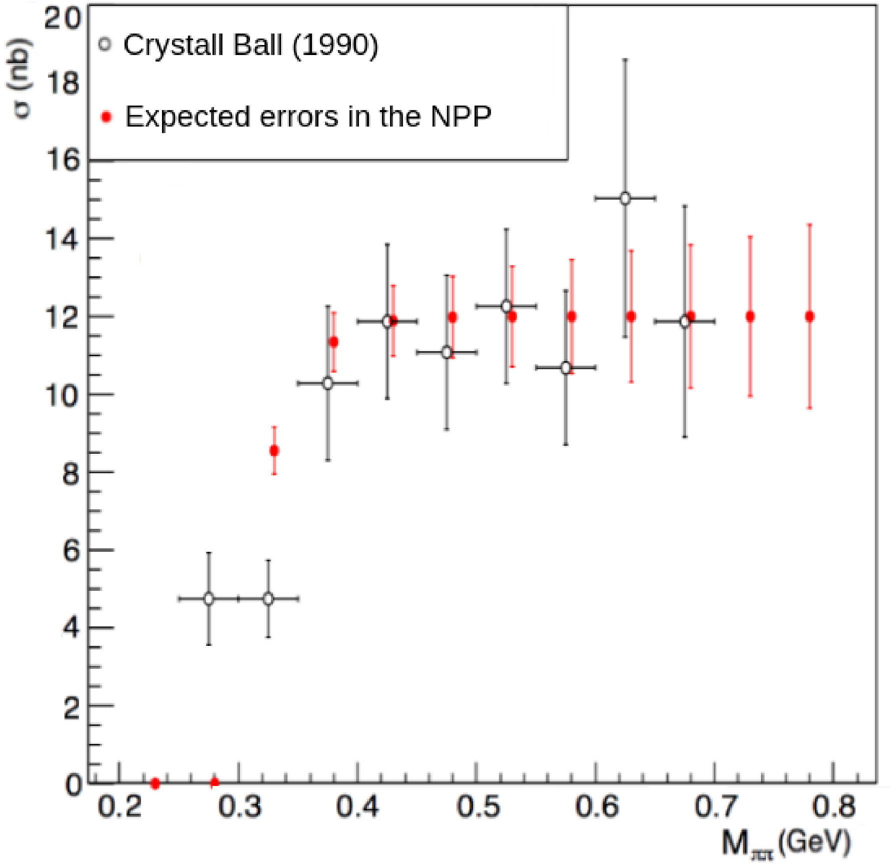

Left: $\gamma\gamma \to \pi^+\pi^-$ cross section. The solid, dashed, dotted curves — model calculation with $\alpha_\pi - \beta_\pi$ — equal to 0,0, 5,7(ChPT) and 13,0 respectively. Black data points are from the MARK-II experiment, The red data points are projected data points for the CPP experiment at Jlab.

Right: Estimated total cross section for $\gamma\gamma \to \pi^0\pi^0$ from NPP(JLab) experiment and data points from the single previous Crystal Ball measurement (disadvantage here is a very low statistics ~300 events collected for the reaction $\gamma\gamma\to\pi^0\pi^0$) .

CPP and NPP experiments at Jefferson Lab

The goal of the CPP and NPP experiments is to make a presicion measurement of pion polarizabilities by collecting of a high statistical data set of the $\gamma\gamma^* \to \pi^+\pi^-$ и $\gamma\gamma^* \to \pi^0\pi^0$ reactions near the threshold through the Primakoff process (pion photoproduction in the Coulomb field):

$$\frac{d^2\sigma_{Pr}}{d\Omega_{\pi\pi} dM_{\pi\pi}} = \frac{2\alpha Z^2}{\pi^2} \frac{E_\gamma^4 \beta^2}{M_{\pi\pi}} \frac{sin^2\theta}{Q^4} |F(Q^2)|^2 (1 + P_\gamma cos2\phi_{\pi\pi}) \sigma(\gamma\gamma \to \pi\pi)$$

Where σ_{Pr} — is the Primakoff cross section of two pions production, $\Omega_{\pi\pi}$ is the solid angle in the laboratory frame for the emission of the 2π system, $M_{\pi\pi}$ is the invariant mass of the 2π system, E_γ is the energy of the incident photon beam, Z is the target atomic number, β is the velocity of the 2π system, P_γ is the linear polarization of the incident beam, $\phi_{\pi\pi}$ is the azimuth angle of the 2π system, F(Q) is the electromagnetic form factor of the target, θ is the lab angle for system, **and $\sigma(\gamma\gamma \to \pi\pi)$ is a total cross section which is sensitive for the pion polarizability**.

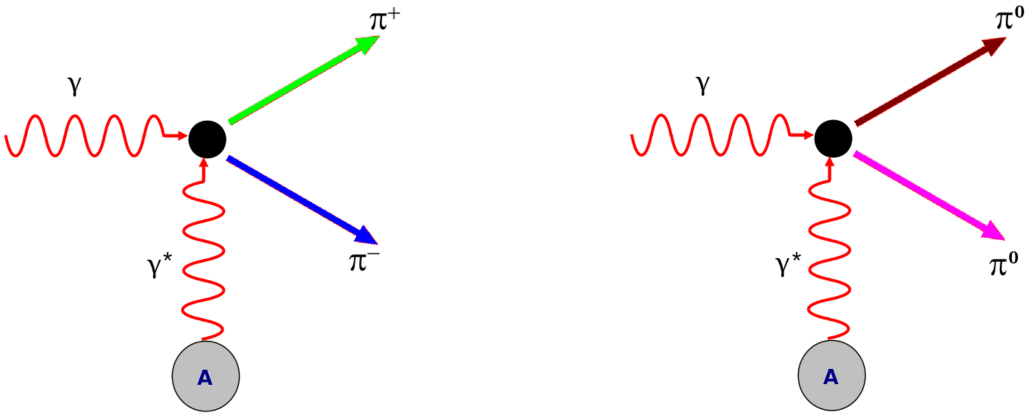

CPP/NPP experimental layout (GlueX setup upgrade)

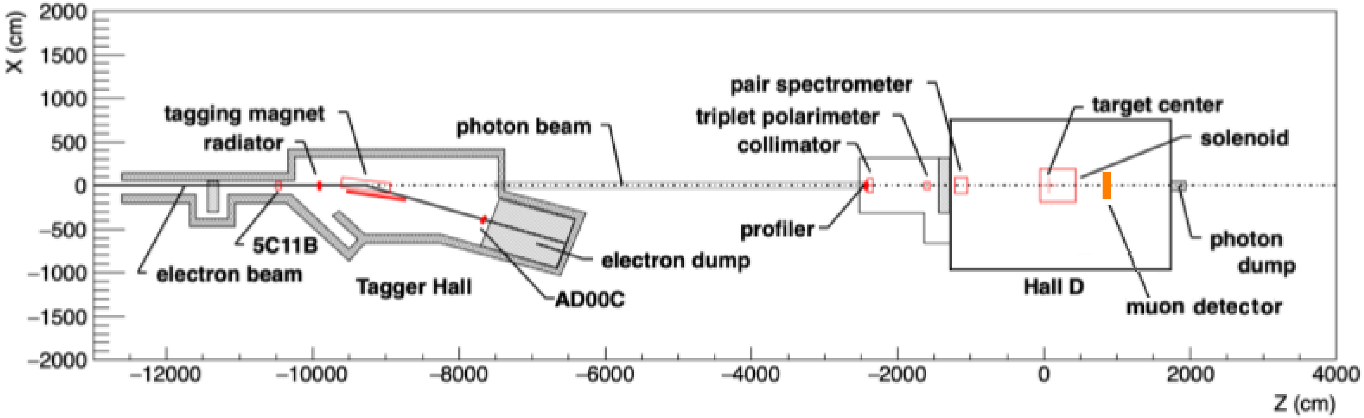

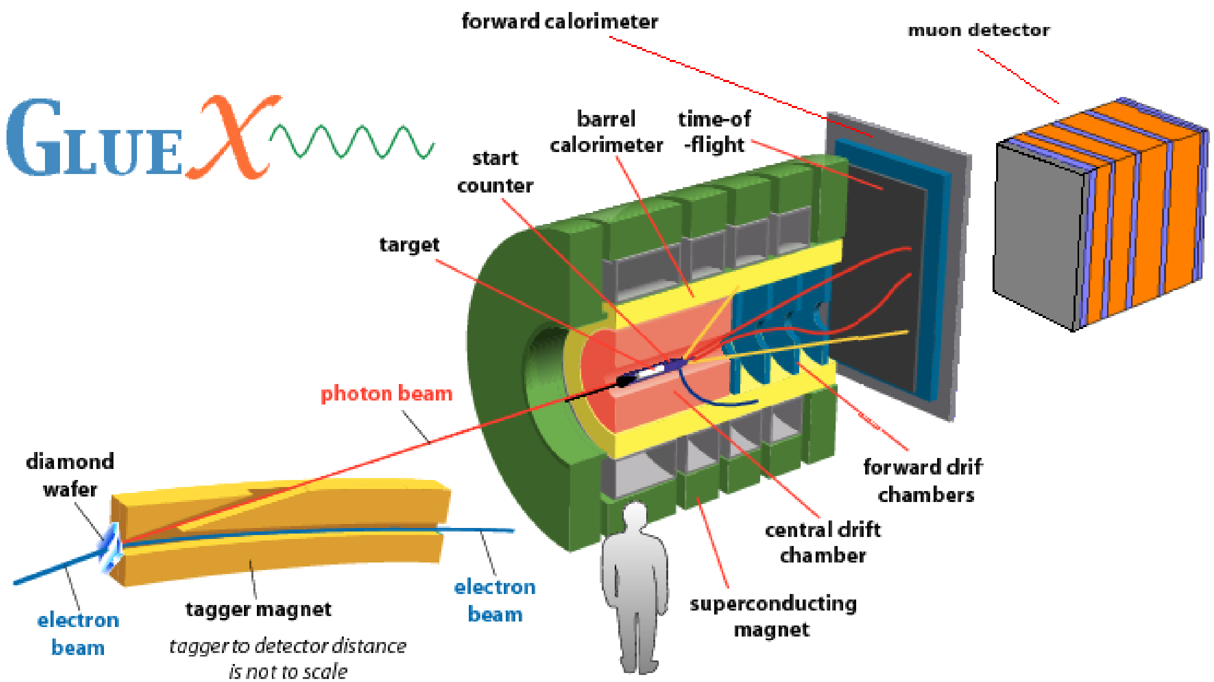

Modification to the GlueX setup:

- **Muon detector** for separation pion and muon pairs
- **Lead target (5% rad. length),** to increase Primakoff photoproduction
- **DIRC** and **start counter** were **excluded**
- **New trigger** based on TOF

Muon detector (was used only for the CPP experiment)

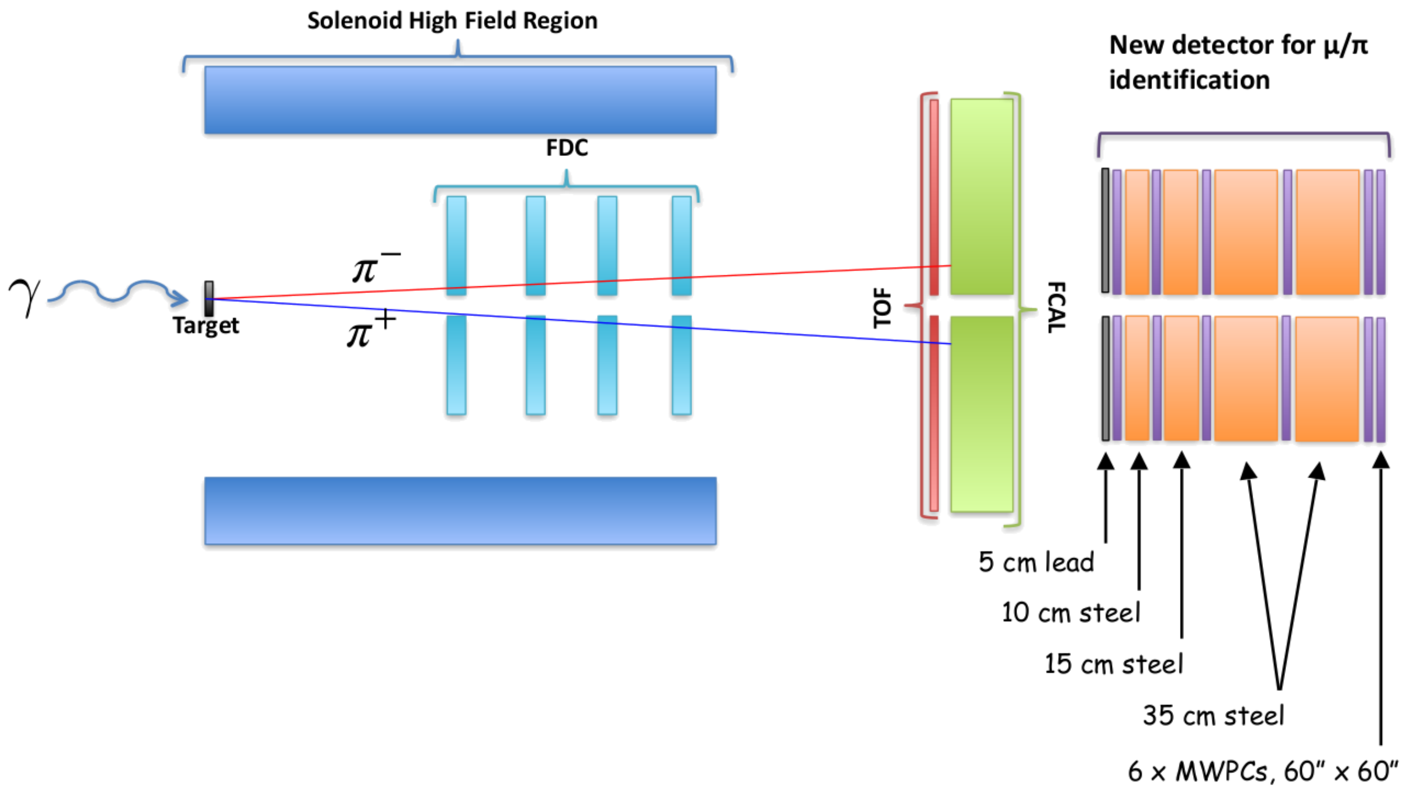

Muon detector was installed right after forward calorimeter (FCAL)

Clarification for the NPP experiment: no additional equipment was required for the GlueX setup - gamma quanta from π0 decays were detected using the forward (FCAL) and barrel (BCAL) calorimeters

Experimental conditions

- The requirements for experiments measuring the polarizability of neutral and charged pions are identical
- Large Z target number → signal amplitude is proportional to Z^2
- Reduced beam energy (relative to the standard one in the GlueX experiment) → 5-5.5 GeV gives better acceptance and higher polarization (electron beam energy ~11.4 GeV)

Setup configuration	GlueX	CPP	NPP
Beam energy, GeV	8.4-9.0	5.5-6.0	5.5-6.0
Beam current, nA	150	20	20
Beam polarization, %	35	72	72
Target position, cm	65	1	1
Target, length in cm	liquid hydrogen, 30	Lead-208, 0.028	Lead-208, 0.028
Muon detector	No	Yes	Yes (not used)
Trigger	FCAL/BCAL	TOF	FCAL/BCAL

Singe π^0 and η layouts using preliminary calorimeter calibration (2022)

$\pi^0 \to \gamma\gamma$, gamma beam energy is 4.5-6.0 GeV

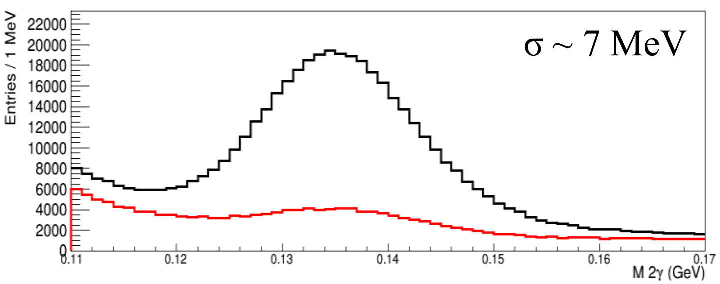

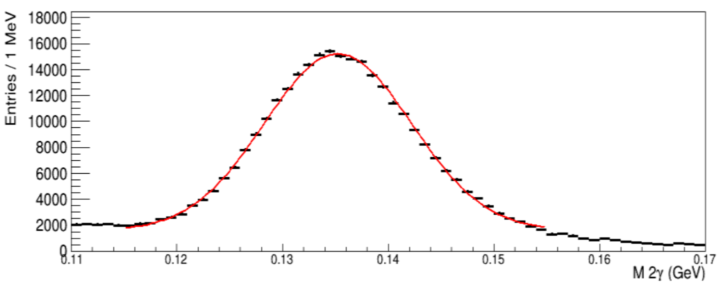

$\eta \to \gamma\gamma$, gamma beam energy greater than 8 GeV

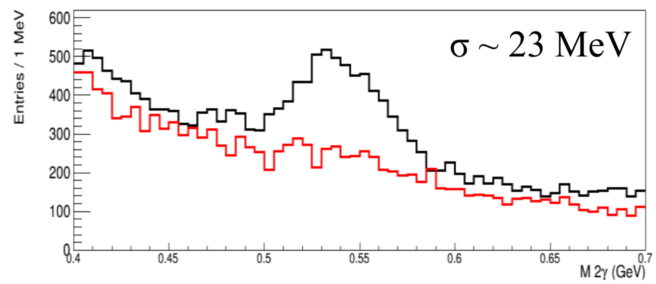

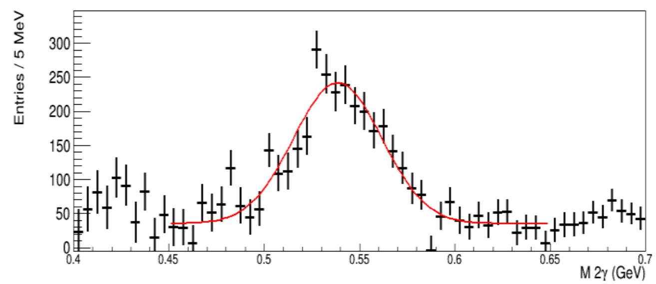

Energy screen (from shifts)

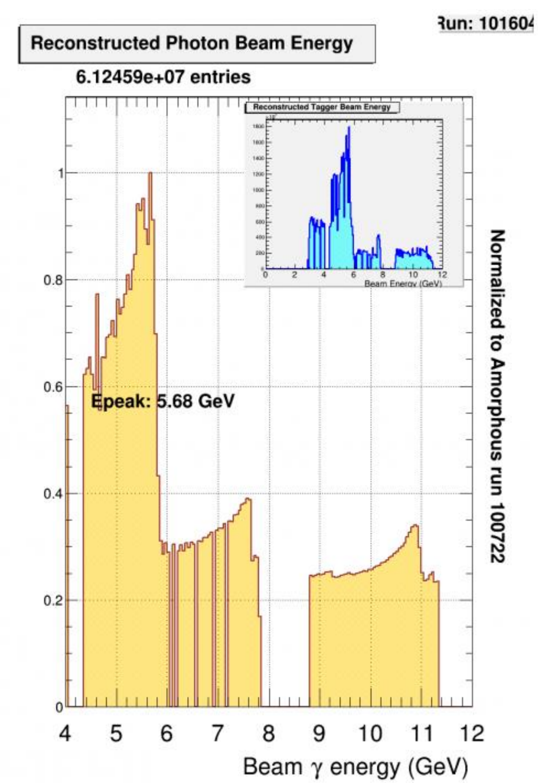

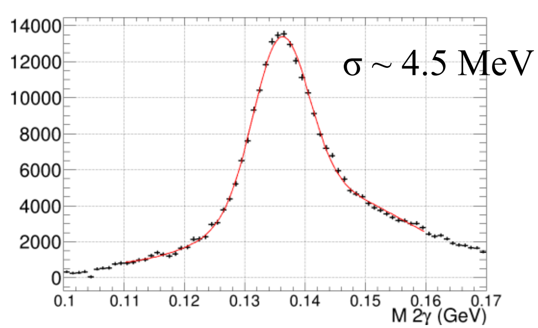

Lead target

Without target

$\pi^0 \to \gamma\gamma$ «elastic part», very preliminary

π0 yield, Pb target, $\gamma Pb \rightarrow \pi^0 \rightarrow \gamma\gamma$
(preliminary and partial statistics)

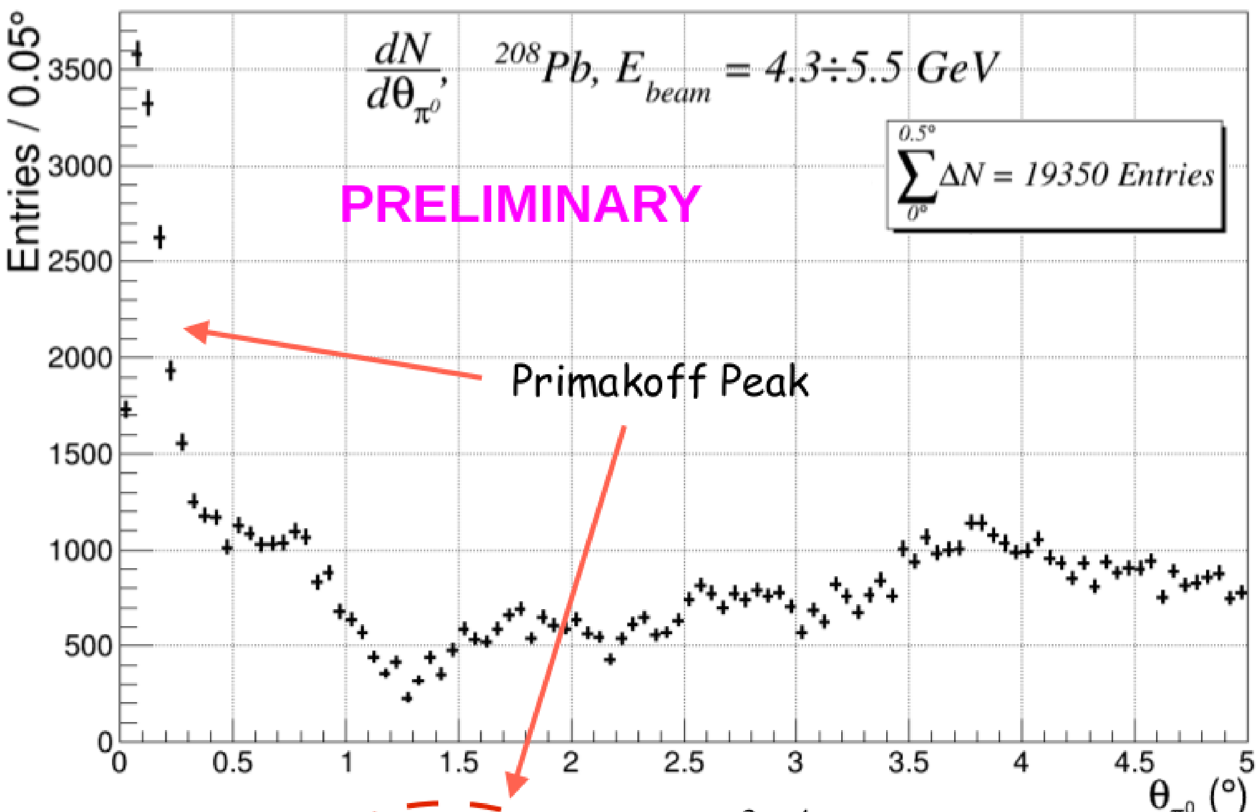

$$\frac{d\sigma_{Prim}}{d\Omega} = \Gamma(\pi^0 \rightarrow \gamma\gamma)\frac{8\alpha Z^2}{m_\pi^3}\frac{\beta^3 E_\gamma^4}{Q^4}\left|F_{EM}(Q^2)\right|^2 sin^2\theta_\pi$$

PrimEx-I
$\gamma Pb \rightarrow \pi^0 Pb$

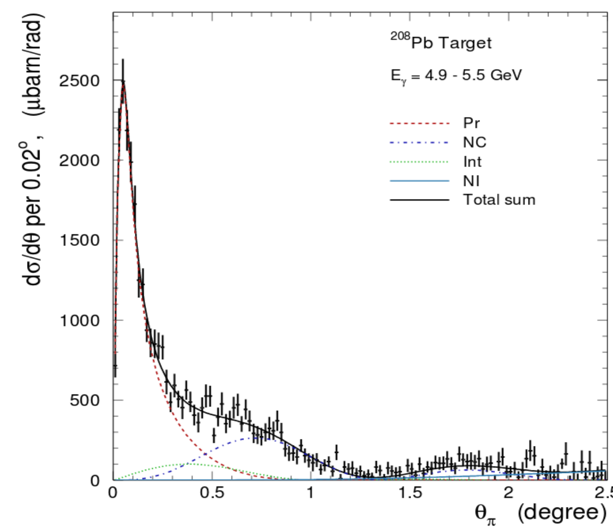

Larin I. et al. (PrimEx Collaboration) Phys. Rev. Lett. 2011. V. 106. P. 162303.

η yield, Pb target (reaction $\gamma Pb \to \eta \to \gamma\gamma$)
(preliminary and partial statistics)

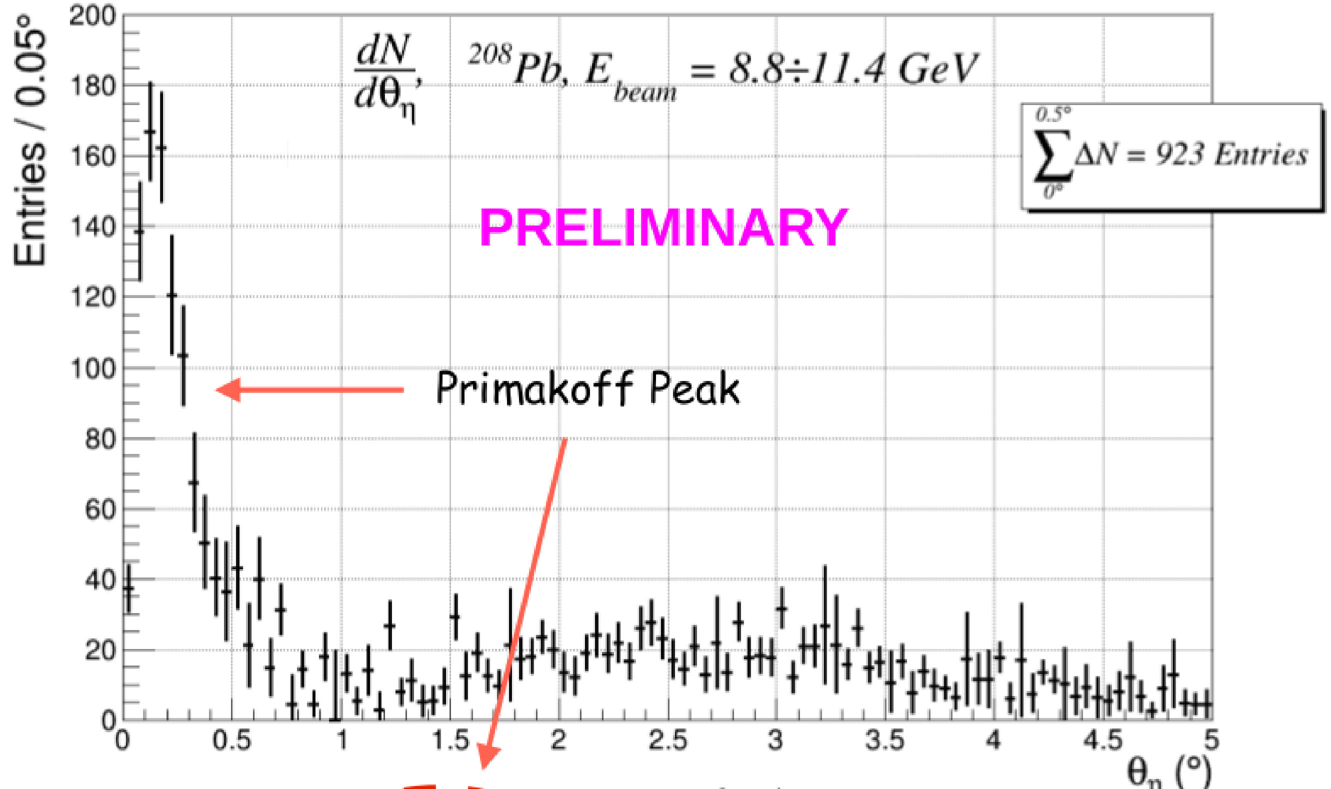

$$\frac{d\sigma_{Prim}}{d\Omega} = \Gamma(\eta \to \gamma\gamma)\frac{8\alpha Z^2}{m_\eta^3}\frac{\beta^3 E_\gamma^4}{Q^4}\left|F_{EM}(Q^2)\right|^2 sin^2\theta_\eta$$

Very preliminary look at ω^0 photoproduction in the reaction $\gamma Pb \to \pi^+ \pi^- \pi^0$

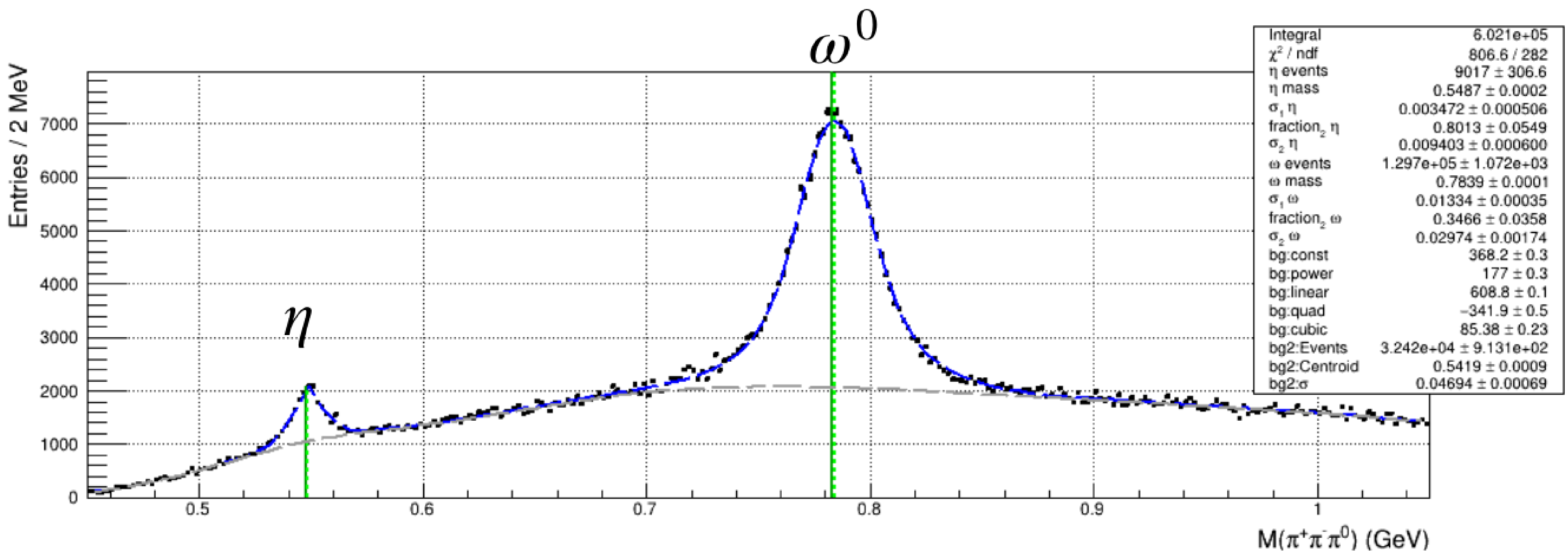

$\pi^+\pi^-\pi^0$ invariant mass

$2\pi^0$ system (preliminary and partial statistics)

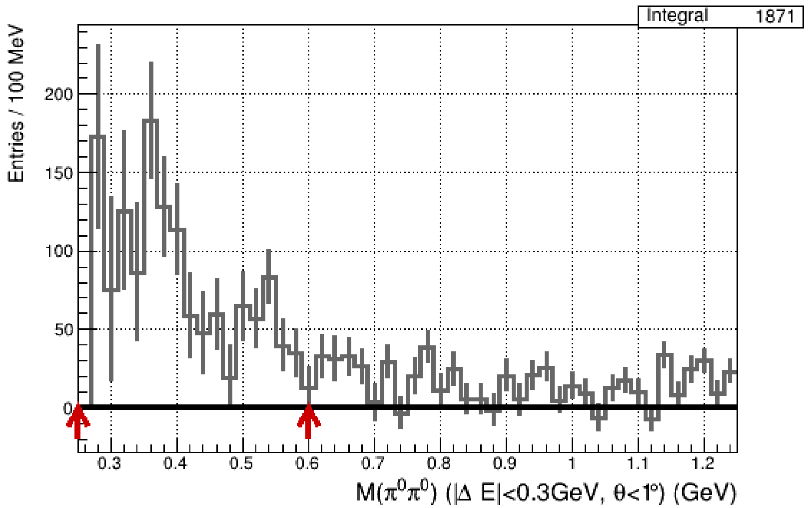

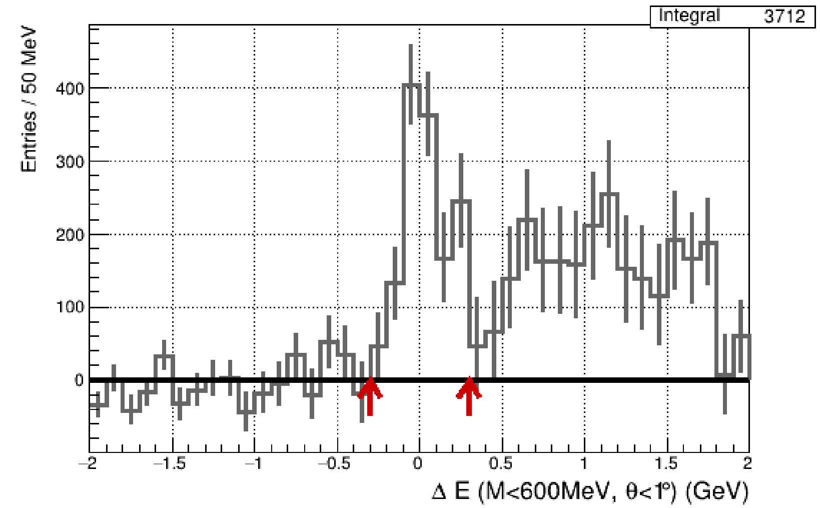

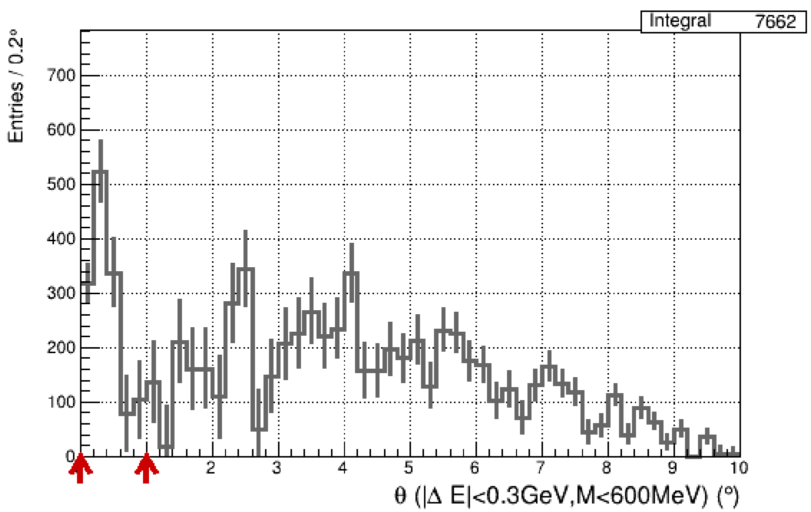

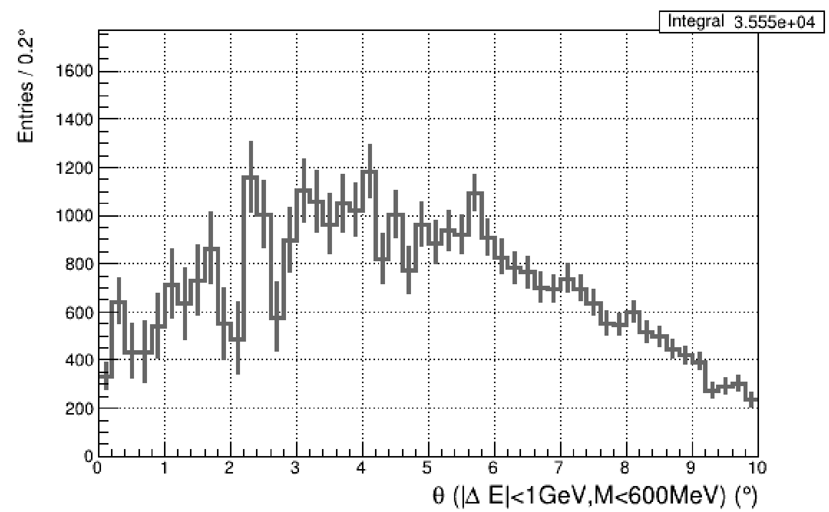

ΔE — difference between incident gamma beam energy and energy of $2\pi^0$ system
M — mass of the $2\pi^0$ system

$3\pi^0$ system (preliminary and partial statistics)

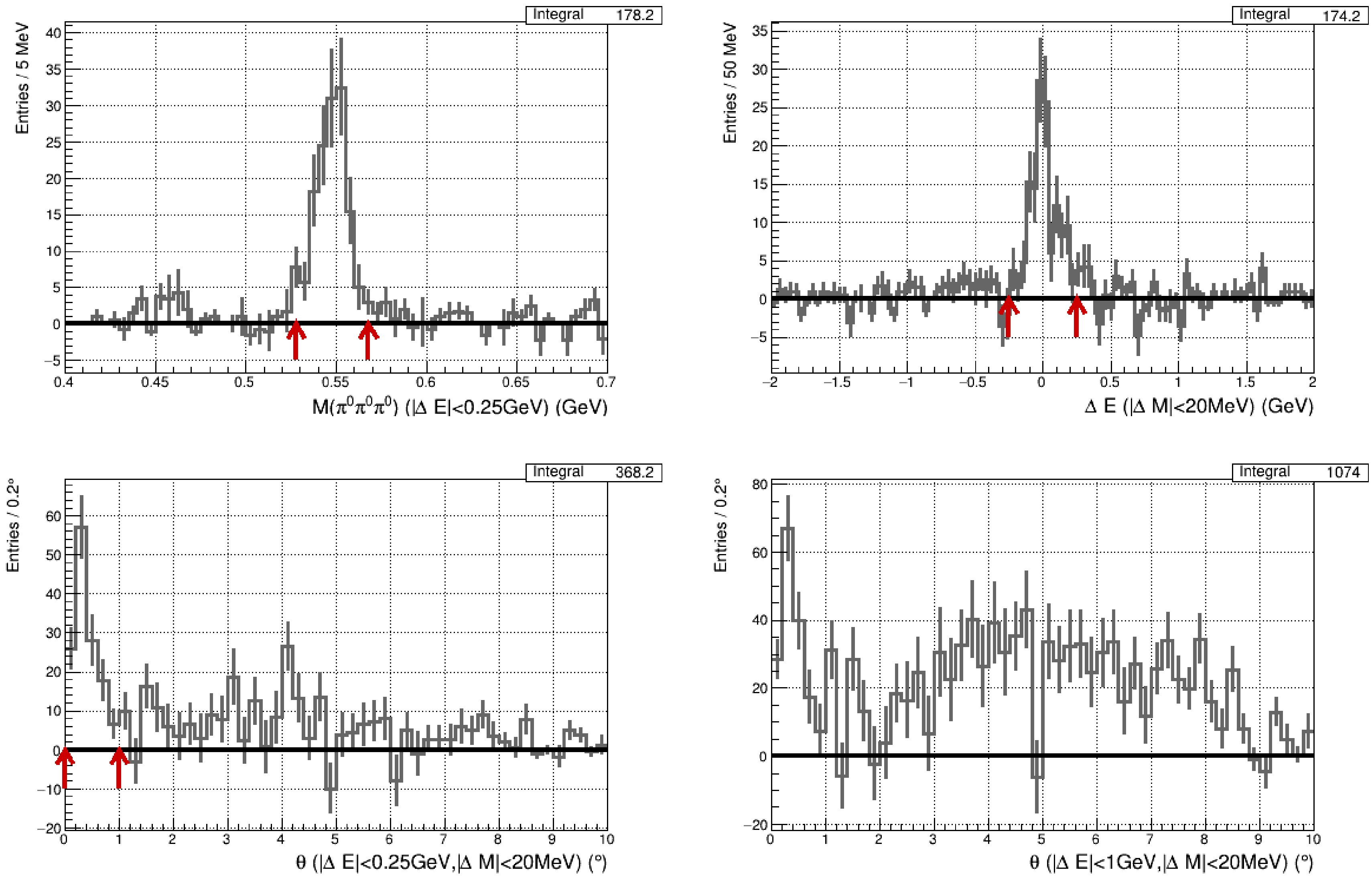

ΔE — difference between incident gamma beam energy and energy of $3\pi^0$ system
ΔM — difference between mass of the $3\pi^0$ system and η mass

Conclusion

- In the summer of 2022, data were collected to measure the polarizability of a charged pion at the Thomas Jefferson Laboratory in Hall D.
- In parallel, statistics were collected to measure the polarizability of the neutral pion.
- A total of 106 billion events were collected on the lead-208 target. 23 billion events were collected without a target for background analysis.
- All calibrations for neutral and charged particles have beed done.
- Working on the convertion from the raw data to data suitable for processing and analisys.
- Preliminary results are planning to recieve later this year or at the beginning of the next year.

Thank you!

Vasiliy Polenov, Grandma's garden, 1878.
Tretyakov Gallery, Moscow, Russia

Additional slides

Hadronic Light-by-Light and the Pion Polarizability

Kevin T. Engel,[1] Hiren H. Patel,[2] and Michael J. Ramsey-Musolf[3]

[1] *California Institute of Technology, Pasadena, CA 91125 USA*
[2] *Department of Physics, University of Wisconsin, Madison, WI 53706, USA*
[3] *Department of Physics, University of Wisconsin, Madison, WI 53706, USA and Kellogg Radiation Laboratory, California Institute of Technology, Pasadena, CA 91125*

We compute the charged pion loop contribution to the light-by-light scattering amplitude for off-shell photons in chiral perturbation theory through next-to-leading order (NLO). We show that NLO contributions are relatively more important due to a fortuitous numerical suppression of the leading-order (LO) terms. Consequently, one expects theoretical predictions for the hadronic light-by-light (HLBL) contribution to the muon anomalous magnetic moment, a_μ^{HLBL}, to be sensitive to the choice of model for the higher momentum-dependence of the LBL amplitude. We show that models employed thus far for the charged pion loop contribution to a_μ^{HLBL} are not consistent with low-momentum behavior implied by quantum chromodynamics, having omitted potentially significant contributions from the pion polarizability.

In this spirit, we have analyzed the charged pion loop contribution to the LBL amplitude to NLO and have compared with corresponding predictions implied by models used in the computation of a_μ^{HLBL}. The leading order (in chiral counting) contribution is fixed entirely by gauge invariance and contains no unknown constants. As we show below, this contribution is fortuitously suppressed. As a result, higher order contributions are likely to be relatively more important than one might expect on general grounds, rendering this quantity more susceptible to model-dependent uncertainties. Thus, it becomes all the more important that any model used for the charged pion contribution to a_μ^{HLBL} respect the requirements of QCD at NLO in the low-momentum regime. In this respect, we find that models utilized to date have omitted a potentially significant contribution associated with the pion polarizability, leading one to question the reliability of the presently-quoted value for a_μ^{HLBL}. Below, we provide details of the calculation leading to this conclusion.

K. Engel, H. Patel, M. Ramsey-Musolf, Phys. Rev. D 86, 037502, 2012.

Diagrams of the other π^0 production mechanisms

π^0 Forward Photoproduction off Complex Nuclei (theoretical models)

- Coherent Production $\gamma + A \to \pi^0 + A$

Leading order processes:

(with absorption)

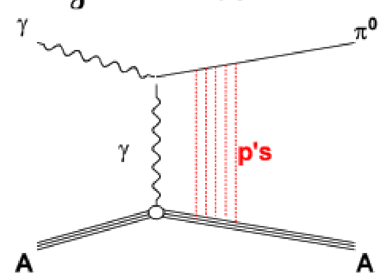

Primakoff

+

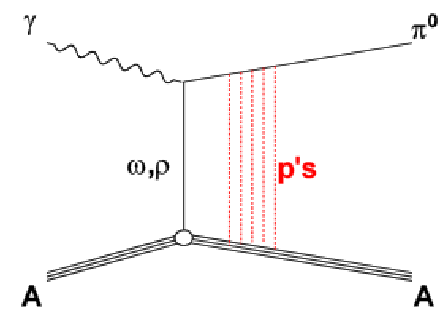

Nuclear coherent

Next-to-leading order:

(with absorption)

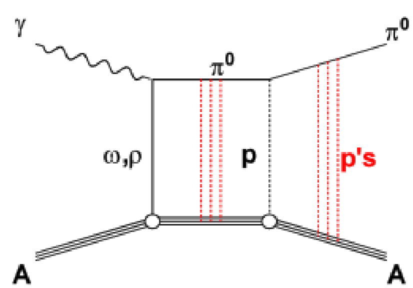

π^0 rescattering

+

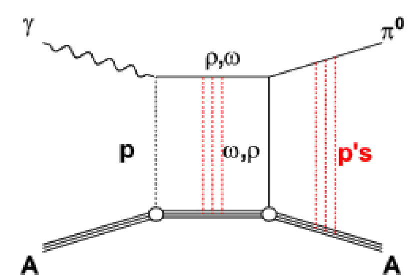

Photon shadowing

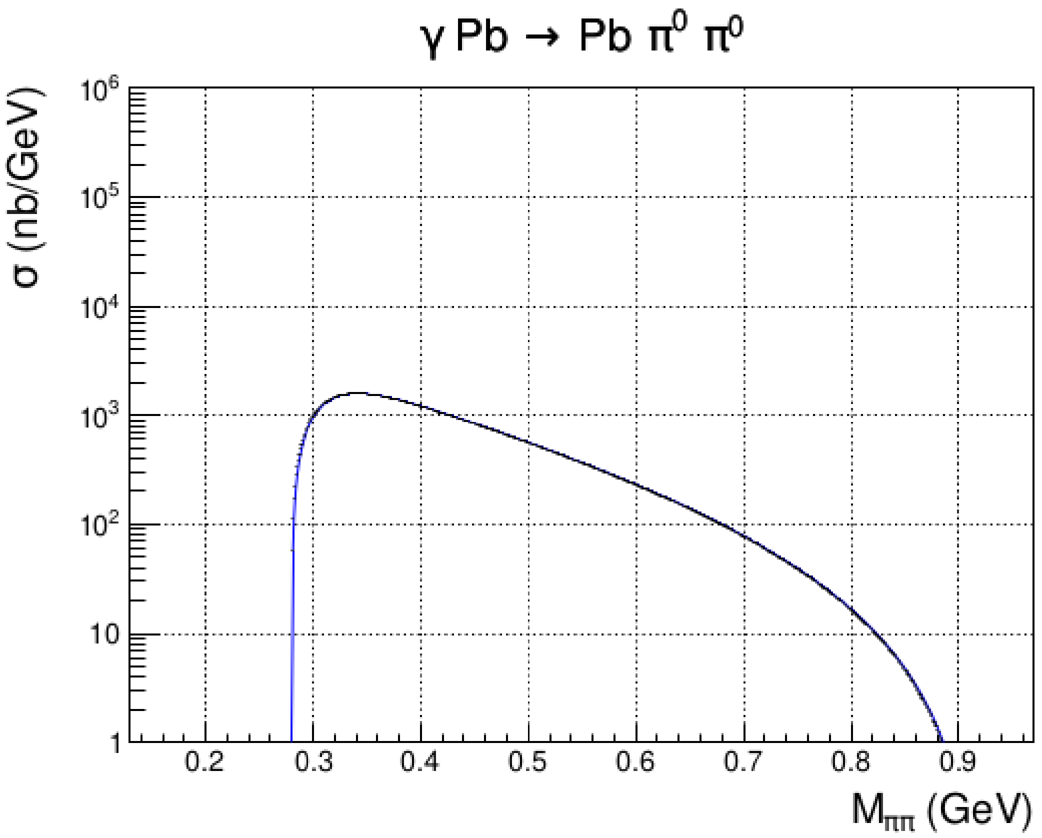

The calculated Primakov cross section[1] for $\gamma Pb \rightarrow Pb\pi^0\pi^0$ using the CPP/NPP setup configuration and the $\sigma(\gamma\gamma \rightarrow \pi^0\pi^0)$ parameterization, which was measured with limited statistical accuracy by the Crystall Ball collaboration[2].

[1] M. Ito et. al., Measuring the Neutral Pion Polarizability. Proposal Submitted to PAC 48, 2020.
[2] H. Marsiske et al. Phys. Rev., D41:3324, 1990.

Coherent bremstrauhlung (photon) beam

Coherent bremstrauhlung is observed experimentally when electrons traverse crystalline targets

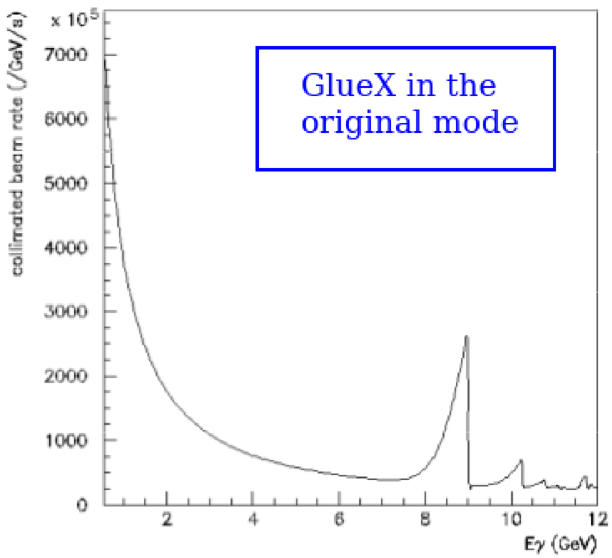

Figure 5: Collimated beam rate at 9 GeV. The ratio of events in the peak (8–9 GeV) to events outside the peak is 0.068.

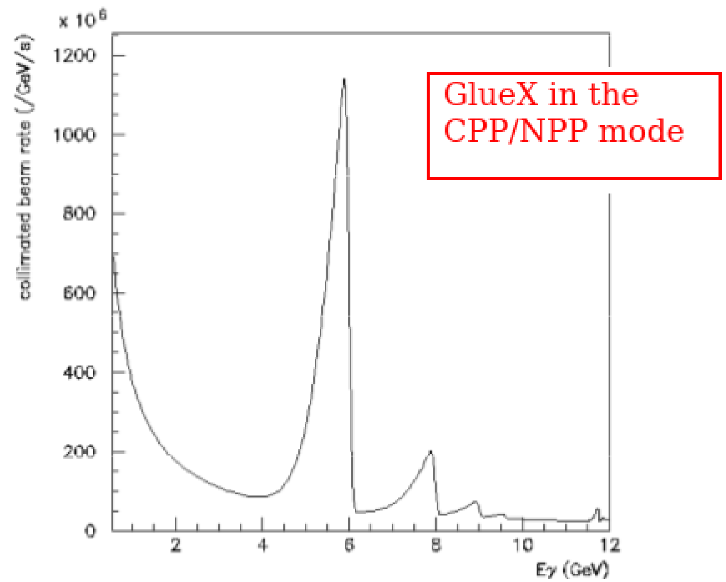

Figure 6: Collimated beam rate at 6 GeV. The ratio of events in the peak (5–6 GeV) to events outside the peak is 0.32.

AlekSejevs A., Barkanova S., Dugger M. et. al. A proposal to the 40 th Jefferson Lab Program Advisory Committee.
https://www.jlab.org/exp_prog/proposals/13/PR12-13-003.pdf

Forward calorimeter

· The Forward calorimeter consists of 2800 lead glass modules sized 4x4x45 cm^3 for the identification of gammas from the decays of the π-mesons.

· Located at a distance of 5.6 meters from the target.

· Central 3x3 modules hole.

· Energy resolution for gammas: $6\%/\sqrt{E} \pm 1.6\%$.

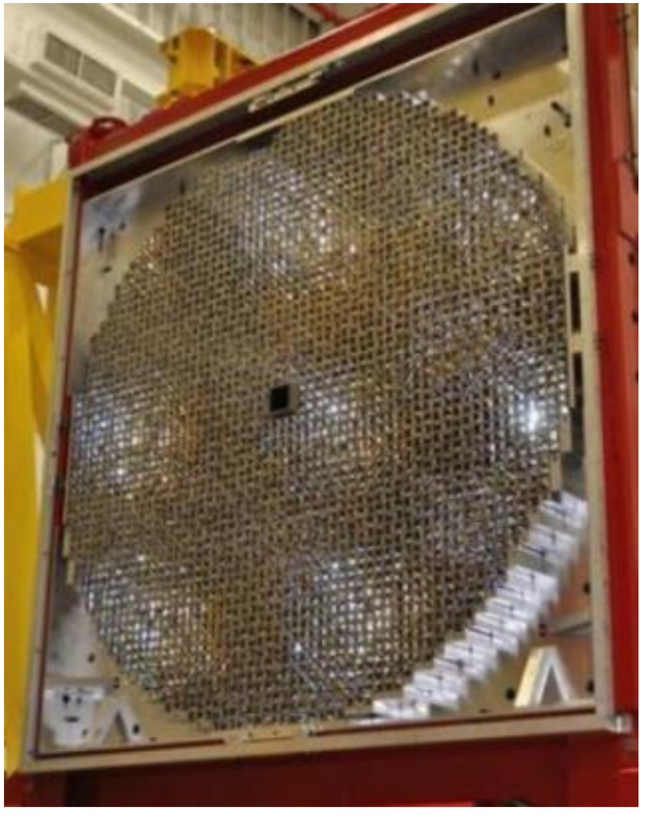

5.5 Lepton Pair Backgrounds

To compare relative rates for $\gamma A \to e^+e^-A$, $\gamma A \to \mu^+\mu^-A$ and $\gamma A \to \pi^+\pi^-A$, it is convenient to calculate cross sections for $\gamma\gamma \to e^+e^-$, $\gamma\gamma \to \mu^+\mu^-$ and $\gamma\gamma \to \pi^+\pi^-$. The angular distributions are shown in Fig. 16, where the lepton pair cross sections are derived from expressions in Bjorken and Drell. The $\pi^+\pi^-$ pair cross sections are from the MARK II data [Bo92]. The red, green and blue curves are for $\mu^+\mu^-$, $\pi^+\pi^-$ and e^+e^-, respectively, and the solid, dashed, and dash-dot curves are for CM energies of 300, 400, and 500 MeV. Over the angular range from 40 to 140 degrees, where GlueX has relatively good angular acceptance, the e^+e^- rate is negligible, and the muon:pion ratio can range from approximately 10:1 to 1:1. Because of the high muon rate relative to the pion rate, it will be necessary to instrument GlueX with a forward angle muon veto counter placed behind FCAL. Details of the detector system are given in Appendix A.

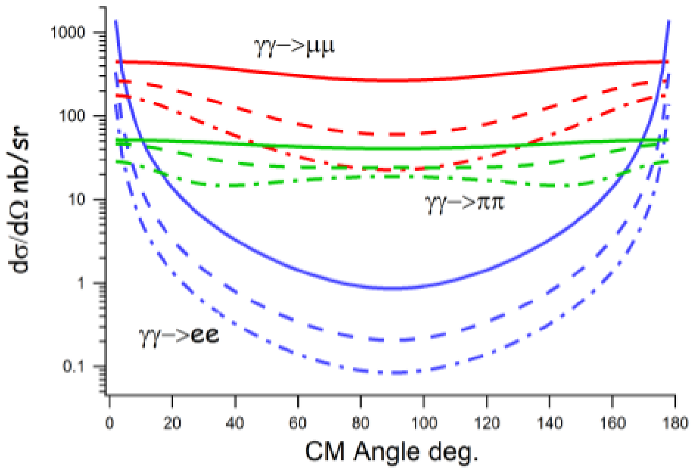

Figure 16: Angular distributions for e^+e^-, $\mu^+\mu^-$ and $\pi^+\pi^-$ pairs are shown as red, green and blue curves, respectively. The solid, dashed, and dash-dot curves are for 300, 400 and 500 MeV CM energies.

A. AlekSejevs et. al. A proposal to the 40 th Jefferson Lab Program Advisory Committee. https://www.jlab.org/exp_prog/proposals/13/PR12-13-008.pdf

Dependence of the polarization of a photon beam on its energy

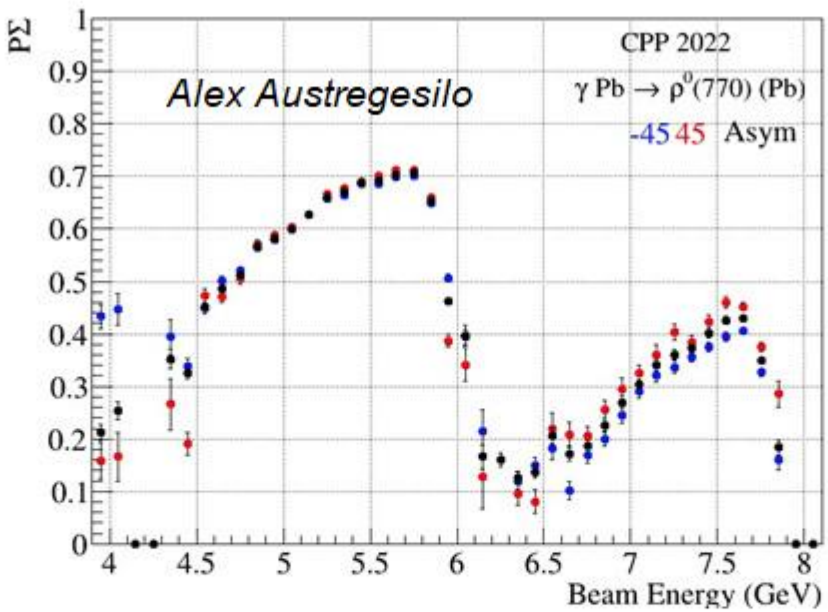

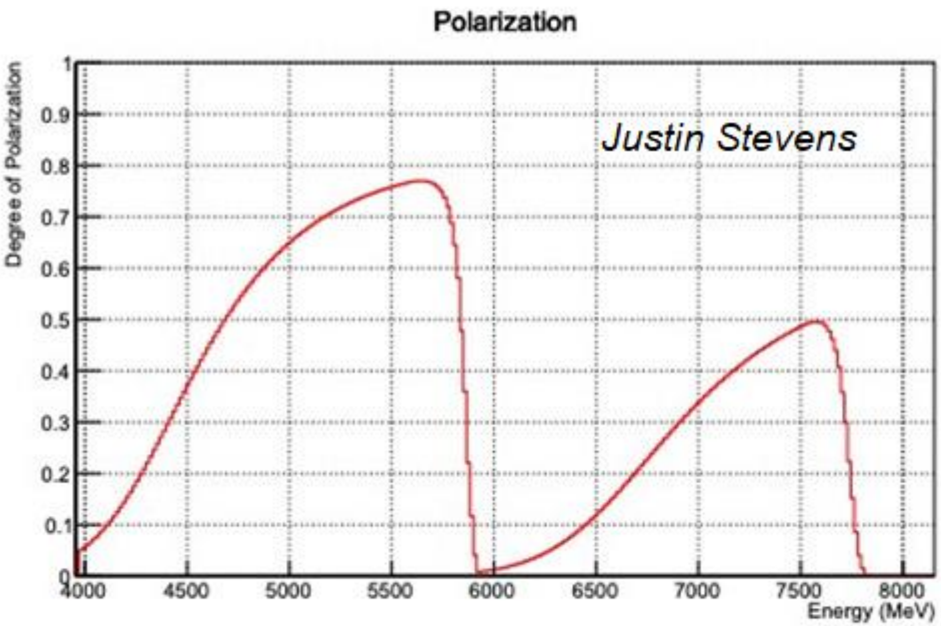

Information on the degree of polarization of the photon beam is obtained by analyzing the azimuthal distribution of scattered atomic electrons in the beryllium target foil using a triplet polarimeter (TPOL).

Monitoring histograms during a run (example)

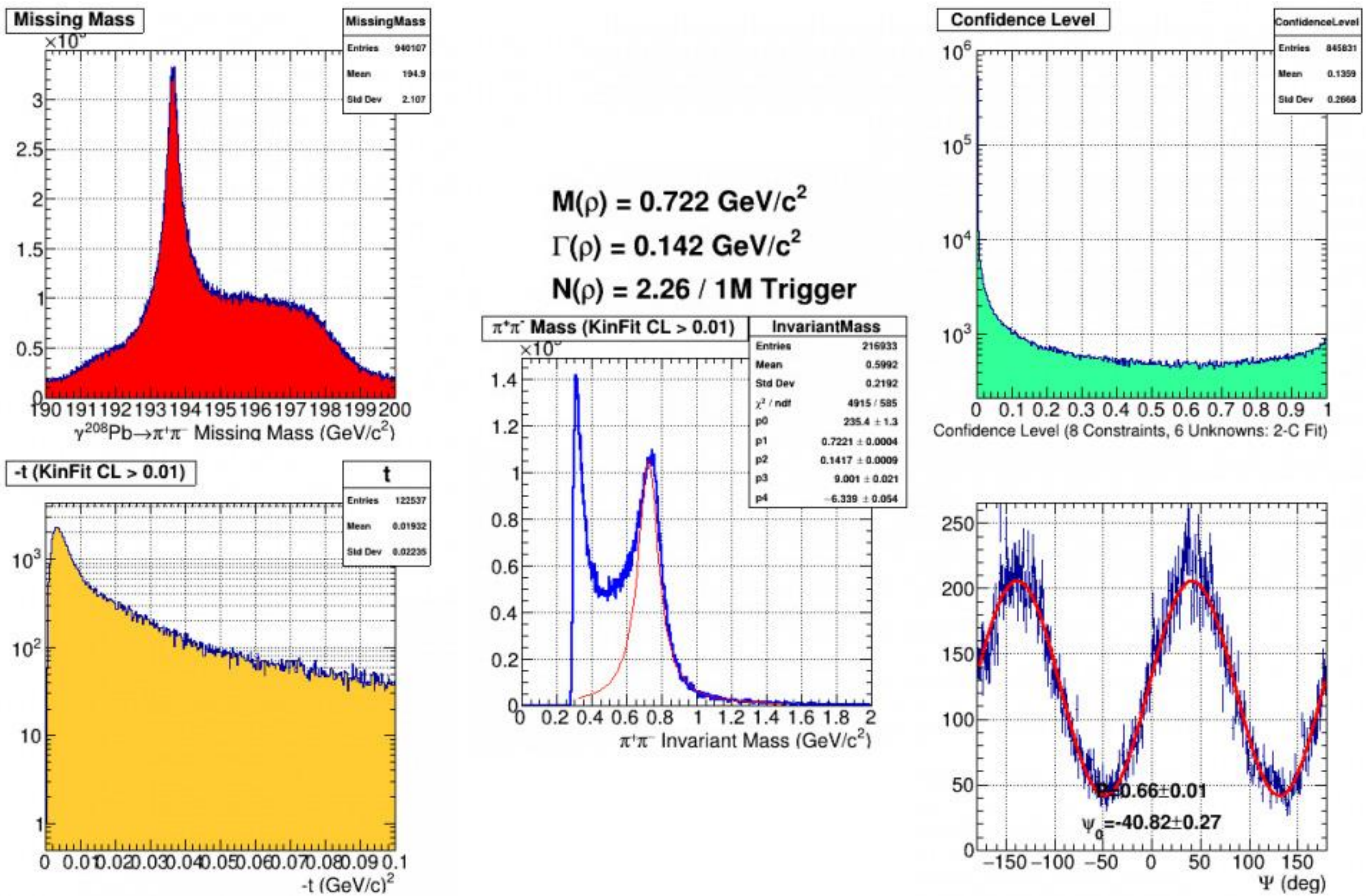

Collected statistics (number of events accumulated vs day of session)

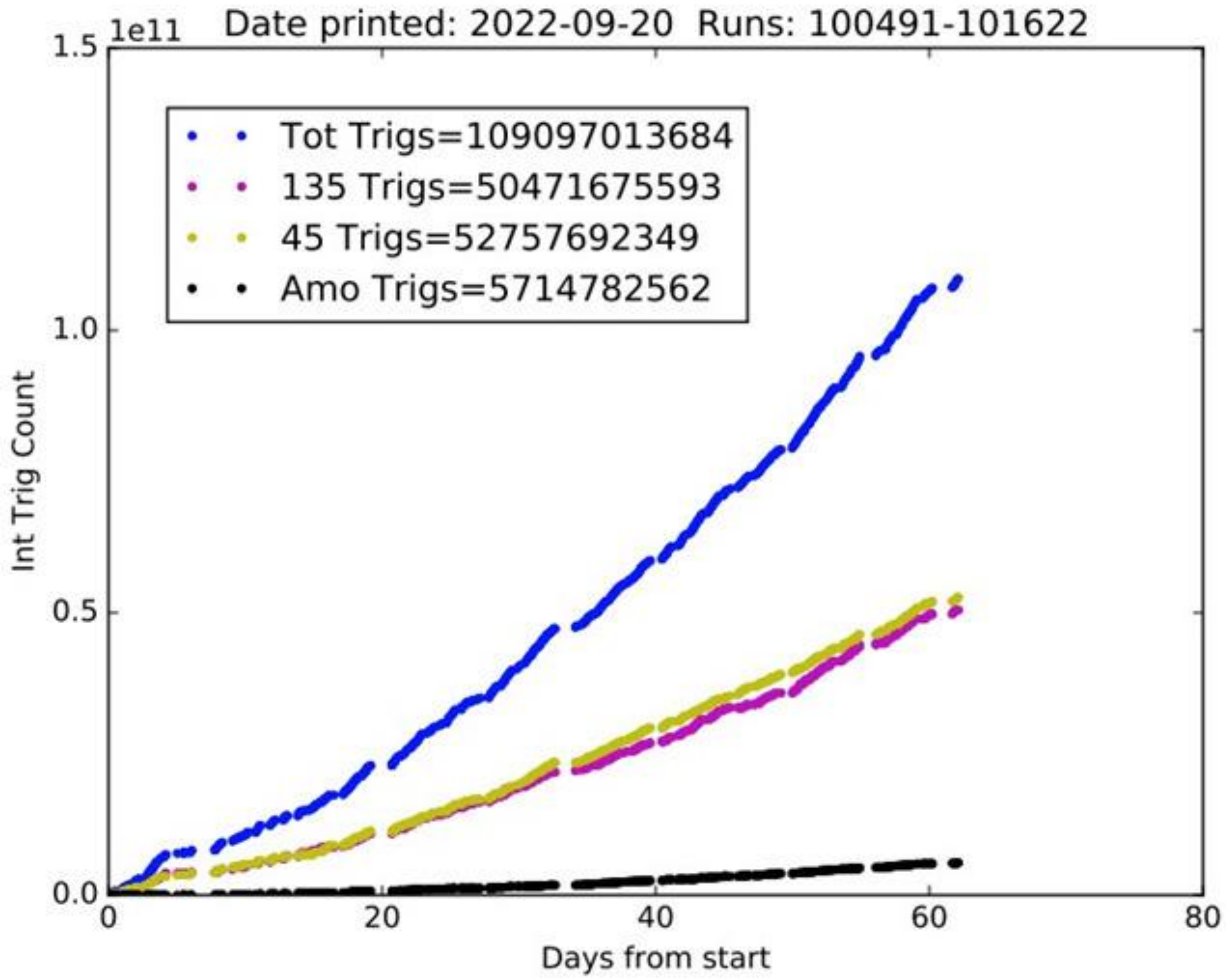

Experimental statistics collected by ~62 days of the session (the session lasted 71 days in total)